Time-resolved absorption and fluorescence from the bacteriorhodopsin photocycle in the nanosecond time regime

J. K. Delaney, T. L. Brack, and G. H. Atkinson
Department of Chemistry and Optical Science Center, University of Arizona, Tucson, Arizona 85721 USA

ABSTRACT Picosecond transient absorption (PTA) in the 568–660-nm region is measured over the initial 80 ns of the bacteriorhodopsin photocycle. After photocycle initiation with 573-nm excitation (7-ps pulsewidth), these PTA data reflect the formation during the initial 40 ps of two long-recognized intermediates with red-shifted (relative to that of BR-570) absorption bands, namely J-625 and K-590. PTA signals at 568, 628, and 652 nm are unchanged for the remainder of the 80-ns photocycle interval measured, demonstrating that no other intermediates, including the proposed KL, are observable by absorption changes. Picosecond time-resolved fluorescence (PTRF), measured at 740 nm, is initiated by 7 ps excitation of the species present at various time delays after the photocycle begins. PTRF signals change rapidly over the initial 40 ps, reflecting, first, the depletion of the ground state BR-570 population and, subsequently, the formation of K-590. The PTRF signal then decreases monotonically with a time constant of 5.5 ± 0.5 ns from its maximum near a 50-ps delay until it reaches a minimum at a delay of ≈13 ns. For time delays between 13 and 80 ns, the PTRF signal remains unchanged and slightly higher than that measured from BR-570 alone. The rapid decrease in PTRF signals over the same photocycle interval in which the PTA signals remain unchanged suggests that the retinal-protein interactions involving electronically excited K-590 (K*) are being significantly altered.

INTRODUCTION

The elucidation of the molecular events that comprise the bacteriorhodopsin (BR) photocycle requires that the electronic and structural changes occurring in the retinal chromophore and the protein environment be considered simultaneously. Accurately deriving such a molecular mechanism from time-resolved spectroscopic measurements is often difficult given both the fact that each type of spectroscopic measurement is sensitive only to specific types of molecular changes and different experimental conditions are often used from one study to another.

For example, the BR photocycle has largely been defined in terms of ground electronic state properties of retinal as measured with a variety of time resolutions by transient absorption spectroscopy (1–4). Time-resolved vibrational spectroscopy of transient intermediates, mostly resonance Raman (RR) data (5–10) and the vibrational spectra of trapped BR species, mostly low temperature Fourier transform infrared data (11, 12), have been correlated with the transient absorption results. These vibrational data provide structural information on the BR photocycle intermediates that is not directly available from the transient absorption data alone. Similarly, time-resolved fluorescence data (13–15) have been interpreted within the context of the absorption changes but actually monitor different aspects of a molecular mechanism (i.e., excited electronic state properties). Clearly, all of this information must be quantitatively correlated to obtain an accurate molecular description of the photocycle. Such direct quantitative comparisons between different types of spectroscopic data from the BR photocycle, however, are rare.

Address correspondence to Dr. George H. Atkinson, Department of Chemistry, University of Arizona, Tucson, AZ 85721, USA.

Determining even kinetic details within the photocycle from transient absorption remains difficult. Since the absorption spectra of the initial photocycle intermediates (J-625, K-590, KL, and L-550) strongly overlap that of BR-570 (1, 2, 14, 16), there are essentially no experimental opportunities to spectroscopically isolate an absorption signal from one of these transient species. Only when considering the absorption spectrum of M-410 with its deprotonated Schiff base are there large absorption differences relative to BR-570 and the other BR photocycle intermediates (1). Thus, for the initial 10 μs of the photocycle, an individual intermediate is identified only through the deconvolution of transient absorption data on the basis of a specific kinetic model. Currently, several kinetic models describing the photocycle remain under consideration since a variety of equilibria between different forms of a given intermediate (e.g., L_1 and L_2 [17] or M_1 and M_2 [17, 18]) and photo-induced reverse reactions (e.g., K-590 + $h\nu \rightarrow$ BR-570 [19–21]) are apparently present under some conditions. Since different photostationary state mixtures of species can be created via optical perturbations of equilibria and/or photo-induced reverse reactions, variations of the excitation powers and pulsewidths used in transient absorption measurements often prevent quantitative comparisons between different time-resolved studies. Differences in the pH and ionic properties of the BR sample also are recognized to alter transient absorption measurements (22), therefore, comparisons of the transient absorption data must consider variations in these parameters as well.

A BR photocycle based primarily on transient absorption data alone does not necessarily provide a complete view of the molecular processes occurring in either the retinal chromophore and/or the protein environment.

0006-3495/93/05/1512/08 $2.00

Changes in the molecular structure may not significantly alter absorption spectra and, consequently, may pass undetected. Other time-resolved spectroscopic data need to be considered to obtain a more complete molecular description of the photocycle.

Perhaps the clearest example of these points involves the transient absorption evidence suggesting that a separate intermediate, KL, is formed as K-590 transforms into L-550. The initial suggestion was based on ΔA measurements between 600 and 650 nm observed 500 ps and 150 ns after the 532-nm excitation (30 ps pulsewidth) of BR-570 (2). A subsequent study using 4–7-ns pulsed excitation at 532 nm identified similar absorption changes only when the pump and probe temporally overlapped during the $\approx$10-ns cross-correlation time (CCT) of the measurement (16). No ΔA changes were reported for time delays > 10 ns; therefore, the authors concluded that a KL intermediate could be formed within the first 10 ns of the BR photocycle (16).

The intermediate KL also has been described in terms of a change in retinal configuration via picosecond time-resolved resonance Raman (PTR^3) scattering (23). Small differences ($\approx$1–2/cm) in vibrational RR bands (notably the C=C stretching modes) observed at 6, 40, and 200 ps have been assigned to KL (23). The largest shift ($\approx$2/cm) occurs between bands recorded with 40- and 200-ps delays (23). These observations, as well as their interpretations in terms of KL, contradict at least in part earlier PTR^3 results in which vibrational bands assigned to K-590 do not change with respect to either relative intensities or positions throughout the initial 40 ps to 26 ns period of the photocycle (reference 10 and Brack, T., and G. H. Atkinson, unpublished results). There also are inconsistencies with respect to the ΔA results. The reported changes in the PTR^3 spectrum have been associated with a blue shift of the absorbance that is assigned to the K-590 → KL transformation (23). Such a blue-shifted ΔA on the 10–200-ps time scale contradicts the transient absorption results that were used originally to suggest that KL is present between 500 ps and 150 ns (2). No ΔA changes are seen from that study (2) during the initial 50–500-ps period. In addition, no ΔA changes in the 10–200 ps interval that are consistent with a blue shift in absorbance are observed in the data reported either here or previously (1–4).

There have been few studies of the fluorescence properties of the BR photocycle relative to the extensive attention given to transient absorption (and even PTR^3 scattering) and seldom have both absorption and fluorescence signals been measured under conditions that permit quantitative comparisons. The fluorescence quantum yield from BR-570 itself is extremely small ($\approx 10^{-4}$ [24]) as is that from the K-590 intermediate ($\approx 2 \times 10^{-4}$ [13]), the only other photocycle species from which fluorescence has been measured. The fluorescence spectra of BR-570 and K-590 overlap significantly, although the fluorescence maximum of K-590 is shifted 17 nm to the blue relative to that of BR-570 (13). Given this spectral overlap, it is convenient to simultaneously monitor the time-dependent fluorescence intensities from both species at a single wavelength ($\approx$745 nm). Recorded with 7-ps time resolution, such picosecond time-resolved fluorescence (PTRF) measurements monitor the total fluorescence signal from the mixture of stable and transient species present at each time delay.

The corresponding picosecond transient absorption (PTA) data monitor the ground state populations of the same photocycle species. When PTRF and PTA signals are measured under conditions that permit quantitative comparisons, it is feasible to separate changes that occur in the excited electronic states of photocycle intermediates relative to their respective ground state populations. Such comparisons permit new insight into the molecular processes underway during this part of the BR photocycle (e.g., KL).

The PTA and PTRF signals are presented in this study for the initial 80 ns of the BR photocycle. The PTA and PTRF measurements are conducted under experimental conditions that ensure that their respective time dependencies can be directly compared quantitatively. Well-recognized absorption changes are observed during the initial 40-ps interval, reflecting the formation and decay of J-625 and the formation of K-590 (1–4). The 568–652-nm absorbance remains constant over the remainder of the initial 80-ns photocycle interval, indicating a constant K-590 ground state population. Contrary to previous results using longer pulsed excitation (2, 16), the PTA data give no indication that another intermediate is formed (e.g., KL). The PTRF signal also changes rapidly throughout the initial 10-ps period both because of the depletion of the BR-570 ground state and the formation of K-590. Unlike the PTA data, however, the PTRF signal then decreases over the next $\approx$13 ns after which it reaches a constant level near, but measurably above, that from BR-570 only. When compared with the PTA results, the PTRF signals reveal new processes occurring during the 40 ps to 80 ns interval that involve changes in the excited electronic state of K-590 (K*) and are interpreted in terms of retinal chromophore-protein interactions.

MATERIALS AND METHODS

The BR samples examined are suspensions of purple membrane (PM) in distilled water and are prepared from strain S9 of *Halobacterium halobium* using published procedures (25). The pH of the suspension is not adjusted with buffer and is ~6.5. The purity of the PM suspensions is verified by ensuring that the ratio of the absorbances at 280 and 565 nm (A_{280}/A_{560}) is between 1.8 and 2.0. The optical density of the suspensions is between 3 and 4 (at λ_{max}). The BR is light adapted before each experiment by exposing the flowing sample to the emission of an incandescent lamp (60 W) for 20 min.

The instrumentation and procedures used to record the PTRF and PTA signals are described in detail elsewhere (13–15). Briefly, the 532-nm second harmonic output of a mode-locked Nd:YAG laser was used to synchronously pump two cavity-dumped dye lasers operating at 1

MHz repetition rates. The 5–8 ps (FWHM) output pulses of the dye lasers were selected to be either in the 560–621-nm range (Rhodamine 6G) to provide a pump pulse (10 mW average power) or in the 620–665-nm (Rhodamine-640) range to provide a probe pulse (2–6 mW average power). The pulsewidth of each laser output was determined by autocorrelation whereas the temporal overlap and timing jitter between the pump and probe pulses were measured by the cross-correlation time (CCT) (12 ps). Delays between the pump and probe laser pulses were obtained over the initial 5-ns time interval by synchronizing the timing of the two cavity dumpers and by advancing the optical delay line located in the optical path of the probe pulse. The probe laser pulse was delayed over the 13.7–82.2-ns interval by selecting different picosecond pulses from the mode-locked pulse train via electronic adjustments to the cavity dumper used with the pump laser. The pump and probe laser beams were colinearly recombined before they were directed to the sample.

A liquid jet ($\approx$350-μm diameter) of the BR sample flowing at $\approx$20 m/s was formed by mechanically pumping it through a cylindrical glass nozzle. To minimize thermal degradation, the sample temperature was maintained at $\approx$10°C by immersing both the sample reservoir and the pump head in ice water. The 20-μm diameter focus of the pump and probe laser beams in the flowing jet together with the jet velocity and the 1 MHz laser repetition rates ensured that for delays < 100 ns the sample volume exposed to one pair of pump-probe pulses was completely removed from the optical path before the next pair of pulses arrived. For the longer delays used, a small fraction of the sample volume exposed to the pump beam exits the optical path before the arrival of the probe pulse. For example, in the case of the longest delay used in this study (82.2 ns), <7% of the pumped sample was replaced by fresh material before the arrival of the probe pulse.

The PTA data were recorded by monitoring the intensity of the probe laser beam with a photodiode (model HUV-2000B; EG&G Inc., Salem, Massachusetts) after it passed through the sample and was spectrally separated from the pump laser beam by reflection from a grating (2,400 lines/mm).

The PTRF signals were generated when the probe laser pulse arrived at the sample after a specific time delay and thereby induced fluorescence from all species present in the BR photocycle at that time. The fluorescence was collected at right angles to the plane formed by the sample jet and the pump and probe laser beams and was focused onto the slit (1 mm) of a 1-m spectrometer (Spex, model 1704), which imaged the emission onto the face of a cooled photomultiplier tube (PMT) (R-943/02; Hamamatsu Corp., Bridgewater, New Jersey). The signal from the photomultiplier tube was processed by a lock-in amplifier (model SC9502; EG&G Ortec Brookdeal, Oak Ridge, Tennessee), which was referenced to a mechanical chopper placed in the probe laser beam only. This ensured that only fluorescence induced by the probe laser was detected. The spectral bandpass (centered at 745 nm) of the detection system was 1.2 nm. Before reaching the spectrometer, the fluorescence passed through glass cut-off filters (models 2-56, 2-63, and 2-59, Corning Glass Inc., Corning, New York; and models -03FCG109 and 03FCG111; Melles Griot/Ilex Optical, Rochester, New York) to eliminate stray light and Raleigh scattering.

A 1,200 groove/mm grating was used to record the fluorescence spectrum at a fixed time delay. For PTRF measurements, this grating was replaced with a flat, silvered mirror that allowed the entire spectral profile to be detected and, thereby, the total fluorescence induced by the probe laser pulse at each pump-probe delay to be recorded.

The fluorescence quantum yield of BR-570 at specific wavelength was obtained by measurements with a triple monochromator (Triple-Mate; Spex Industries Inc., Edison, New Jersey) operating with a cooled diode array detector (model 1420 HD; EG&G Reticon, Sunnyvale, California). The subtractive dispersion of this triple monochromator eliminated the need to prefilter the fluorescence and to use phase-sensitive detection. This experimental arrangement was exactly the same as that used to record PTR[3] signals (10). The fluorescence intensity at 745 nm was measured as a function of low-power (1–8 nJ), pulsed laser excitation throughout the 560–660-nm region. The 560–660-nm range was covered by using the pump (yellow) and probe (red) lasers independently as the excitation sources with sufficiently low pulse power to avoid inducing significant photochemistry from BR-570. Since both lasers operated at 621 nm, the fluorescence yields from the two sets of experiments could be normalized. Indeed, the fluorescence signals observed with excitation at 621 nm from both lasers were the same.

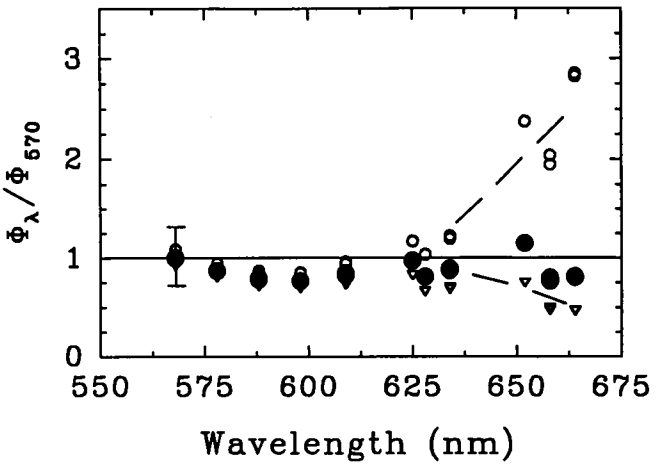

FIGURE 1 Relative quantum yield of fluorescence (Φ_f) from BR-570 as a function of excitation wavelength. Low energy (1–8 nJ/pulse) laser dye laser excitation (7-ps pulses) is used to ensure that no significant BR-570 photochemistry is initiated. The measured fluorescence signal is normalized to the BR absorbance, which is corrected for the contribution to the sample absorbance from the Raleigh scattering associated with the PM fragments. The three data sets reflect different scattering corrections to the measured absorbance: (*i*) the best linear fit to the scatter (*closed circles*), (*ii*) an assumed 30% increase relative to (*i*) in the amount of scatter (*open circles*), and (*iii*) an assumed 30% decrease relative to (*i*) in the amount of scatter (*open triangles*).

RESULTS

Fluorescence yield of BR-570 versus excitation wavelength

The relative fluorescence quantum yield from BR-570 (Φ_λ/Φ_{570}) is shown in Fig. 1 as a function of excitation wavelength (λ) for the 560–660-nm spectral region (Φ_λ is presented normalized to the value at 570 nm, Φ_{570}). Low-power (1–8 nJ) laser pulses excite <1% of the sample at each wavelength, thus ensuring that the fluorescence originates only from the excited electronic state of BR-570 (BR*).

The fluorescence intensity is measured at 745 nm near the maximum in the fluorescence spectrum assigned to BR* (13–15). Since the fluorescence spectra of BR-570 remain unchanged for excitation wavelengths in the 560–660-nm region (*vide infra*), the fluorescence intensity at 745 nm and not the integrated fluorescence band intensity is used to determine Φ_λ/Φ_{570}. Within an experimental error of ±30%, Φ_λ/Φ_{570} (Fig. 1, *filled circles*) does not change for the excitation wavelength between 560 and 630 nm.

The uncertainty in Φ_λ/Φ_{570} increases in the far red (630–660 nm) where the BR-570 absorbance becomes small compared with the scattering contribution to the measured sample absorbance. A quantitative determination of retinal absorption, of course, depends directly on its accurate separation from the scattering. The correct absorption profile of BR-570 can be obtained by subtracting from the measured signal the scattering contribution of the PM fragments. A simple Mie scattering model given by $A\lambda^{-\alpha}$, where A and α are variables, is used to approximate the scattering contributions. The parameters A and α are determined by fitting the BR-570 sample absorbance in a spectral region where scattering from the PM fragments dominates the absorption from the retinal chromophore (e.g., 750–900 nm). Although α varies slightly with BR samples, fits in the 750–900-nm regions give it a value of ≈ 2.

In a spectral region where retinal absorption dominates (e.g., 560–630 nm), the uncertainty of the scattering fit makes little difference. In the 630–660-nm region, however, scattering contributes significantly to the measured sample absorbance and, as a consequence, the uncertainty in the BR-570 absorption increases (typically 50%). Two of the curves shown in Fig. 1 illustrate the effect on Φ_λ/Φ_{570} of a 30% increase (*open circles*) and decrease (*triangles*) in the scattering contributions to the sample absorbance. Clearly, even relatively small changes in the scattering correction can alter Φ_λ/Φ_{570} values in the 630–660-nm region, although there is essentially no effect in the 560–630-nm region. The best linear fit to the Φ_λ/Φ_{570} data (Fig. 1, *filled circles*) exhibits little (<30%), if any, dependence on the excitation wavelength throughout the entire 560–660-nm region.

The BR* fluorescence spectrum in the 700–900-nm region does not vary with laser excitation wavelength for the entire 570–660-nm range used here (data not shown) and is well represented by the spectrum presented previously for 570-nm excitation (13, 15). Measurements of fluorescence spectra with excitation wavelengths > 630 nm, however, require that optical filters with 640–700 spectral cut offs be used to minimize the amount of Raleigh scattering detected. These filters slightly attenuate the fluorescence appearing <700 nm but, more importantly, they can limit how much of the blue edge of the fluorescence can be observed, thereby making it difficult to determine the exact shape of the fluorescence spectrum near the ≈745-nm maximum. Recognizing this limitation, no significant alteration in the blue portion of the fluorescence spectrum is observed as a function of excitation wavelength. The spectral shape of the red half remains unaffected by the filters and is the same for all excitation wavelengths used.

PTA over the initial 80 ns

PTA data recorded during the initial 40 ps of the BR photocycle correspond closely with previously reported results (1–4) in which the formation and decay of J-625

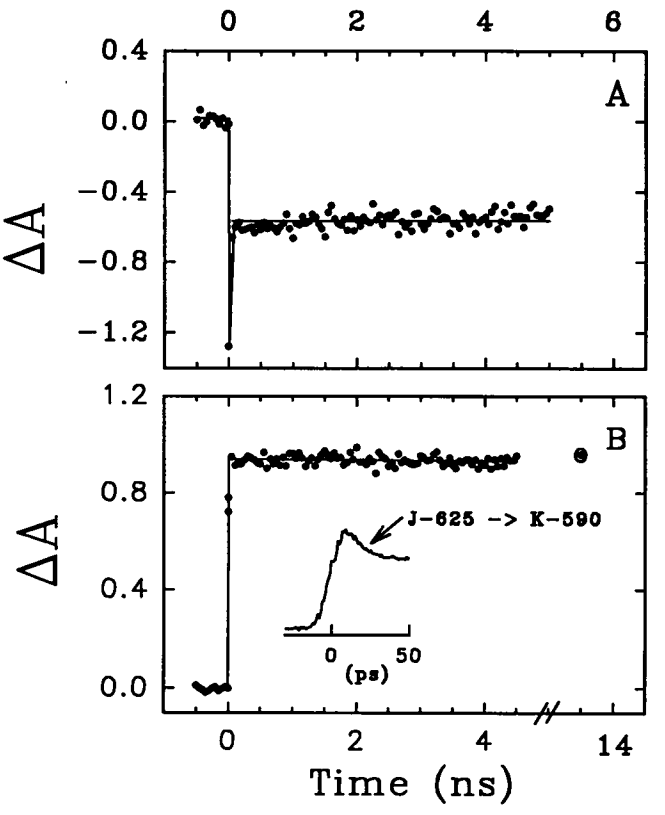

FIGURE 2 PTA changes (ΔA) during the initial 4.5 ns of the BR photocycle after excitation at 573 nm (7-ps pulse) monitored at (*A*) 568 and (*B*) 628 nm. Rapid ΔA changes appear during the initial 100 ps of the BR photocycle at both wavelengths, reflecting the formation and decay of J-625 (within the cross-correlation time) and the formation of K-590 (<40 ps). No changes in ΔA are observed at either wavelength during the 0.1–4.5-ns interval. The data point at 13.7 ns (plotted on a discontinuous time scale in *B*) is obtained using a nanosecond electronic time delay. The inset in *B* shows the ΔA at 628 nm over the 0–50-ps interval. The maximum ΔA value is assignable to J-625 (i.e., $\epsilon_{J\text{-}625} > \epsilon_{K\text{-}590}$ at 628 nm) whereas the decrease in the 10–20-ps interval reflects the J-625 to K-590 transformation.

and the formation of K-590 are clearly observed. With the results of PTA measurements over this time scale confirmed, attention here is given primarily to longer time delays extending to 80 ns. The initial 5-ns interval is measured by continuous scan of the optical delay line whereas longer time delays are obtained by electronic timing *vide supra*.

The PTA during the first 5 ns of the BR photocycle at 568 and 628 nm is shown in Fig. 2 *A* and *B*, respectively. At 568 nm a rapid depletion of the ground state BR-570 population during the 12-ps CCT caused by optical pumping is evident by the decreased 568-nm absorption. The rapid partial recovery of the PTA signal at 568 nm within 20 ps is due to the formation of the K-590 intermediate. From 40 ps to 5 ns, the PTA signal at 568 nm remains constant (±5%). During the 12-ps CCT of the pump and probe laser pulses a positive PTA signal at 628 nm (Fig. 2 *B, inset*) is observed. This rapid ΔA increase is assigned to the formation of the J-625 intermediate.

The decay of J-625 into K-590 appears in the 628-nm signal as a small decrease in absorption before a constant plateau is reached (Fig. 2 *B*, (*inset*). From 40 ps to 5 ns, the PTA signal at 628 nm remains constant (±5%). Similar results to those at 628 nm are observed for a 652-nm probe. The continuous scan of the optical delay at 568, 628, and 652 nm shows that absorbance remains constant (±5%) throughout the initial 5 ns of the photocycle.

The PTA measurements at 628 nm were extended to 80 ns, in increments of 13.7 ns, by using electronic time delays *vide supra*. As is shown in Fig. 2 *A*, no change in absorbance from that measured between 40 ps and 5 ns is observed at 13.7 ns. In addition, no change in absorbance at 628 nm is found between 13.7 and 80 ns. These PTA results indicate that the ground state population of K-590 is constant throughout the initial 40 ps to 80 ns of the BR photocycle.

PTRF over the initial 80 ns

PTRF data ($\Delta I_f/I_f$) measured from the same BR sample and under the same experimental conditions used in the PTA measurements (e.g., pumped at 573 nm and probed at 628 nm) are shown in Fig. 3. The 573-nm PTA data are reproduced in Fig. 3 for comparison. The time-dependent changes in $\Delta I_f/I_f$ over the initial 100 ps are consistent with previously reported results that both revealed the formation of K-590 and indicated that the fluorescence quantum yield from K* is larger (by factor of ≈2) than that of BR-570 (13). There is no evidence that J-625 contributes to the PTRF signals observed.

A dramatic (≈50%) decrease in $\Delta I_f/I_f$ occurs between 100 ps and 13 ns (Fig. 3). The same decay in fluorescence intensity is observed for probe laser wavelengths of 568 and 652 nm (data not shown). A single exponential decay (τ = 5.5 ± 0.5 ns) describes this decrease well (Fig. 3).

The overall change in fluorescence throughout the 80-ns interval measured here can be seen in Fig. 4. The large $\Delta I_f/I_f$ decrease during the initial 4.5-ns interval is again evident whereas for 13–80-ns delays it is clear that the fluorescence remains unchanged at a level above that from the probe laser alone (0.0 in Fig. 4).

Experimentally, the change in fluorescence can not be attributed to rotational diffusion of the PM fragments within the sample jet for two reasons: (*i*) no corresponding change in the ΔA signal is observed that can be associated with the reorientation of the transition dipole moment of the chromophore as would occur for rotational diffusion, and (*ii*) the rotational diffusion time constant of the PM fragments is known to be in the 10^{-2} s regime (26).

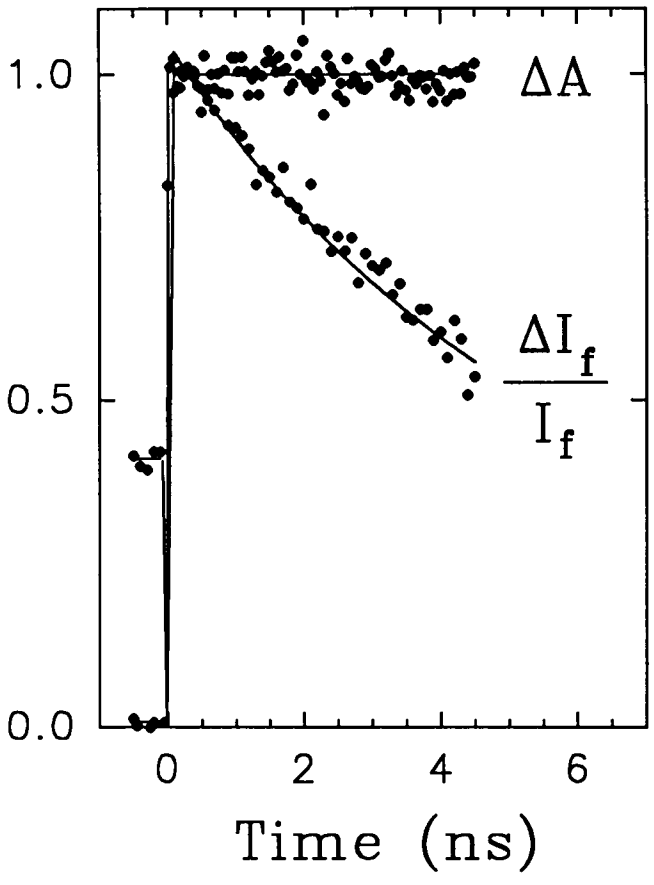

FIGURE 3 PTRF signal ($\Delta I_f/I_f$) during the initial 5-ns interval of the BR photocycle after 573-nm excitation. The PTRF signal is generated by a 7-ps, 628-nm probe pulse. The corresponding ΔA data monitored at 628 nm also are presented on the same time scale. The PTRF signal ($\Delta I_f/I_f$) decreases significantly (≈50%) during the initial 13-ns interval before reaching a constant value. No change occurs in the PTA data over the same 5-ns time period. See text for discussion of photocycle mechanism.

DISCUSSION

A new, more complete view of the molecular events that occur during the 40 ps to 80 ns interval of the BR photocycle can be obtained both from the separate PTA and PTRF data presented here and from their quantitative comparisons. Whereas only absorption changes assigned to specific ground state retinal transitions have been used previously to identify photocycle processes (1–4), the fluorescence results described here expand the definition of photocycle events to include excited state processes. It is well recognized that fluorescence is more sensitive to changes in excited state properties than absorption, but a clear delineation of small fluorescence changes in the BR photocycle requires quantitative comparisons between the PTA and PTRF data acquired under the same experimental conditions. This expanded definition of the BR photocycle in terms of both ground and excited state processes is a task that began with the first picosecond time-resolved detection of fluorescence from K-590 (13).

PTA results

The 600–660-nm absorbance decrease of ≈30% reported previously to occur between 500 ps and 150 ns

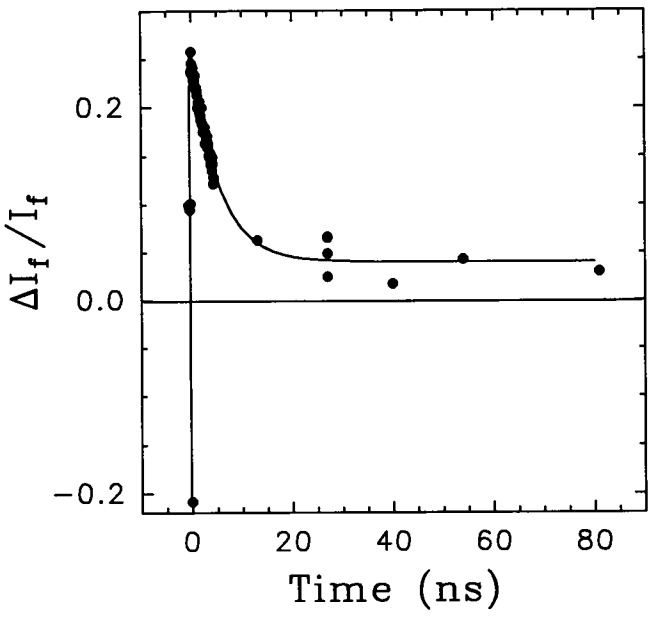

FIGURE 4 PTRF signal ($\Delta I_f/I_f$) during the initial 80 ns of the BR photocycle. The PTRF data for delay times as long as 5 ns are obtained using an optical delay whereas the PTRF data over the 13.7–82.2-ns period are recorded with electronic delays (see text). A large (50%) decrease in fluorescence intensity is observed during the first 13-ns interval while a constant fluorescence signal appears between 13 and 80 ns. These PTRF data are well fit by a single exponential decay having $\tau = 5.5 \pm 0.5$ ns (*solid line*). The PTA signal (monitored at 628 nm) over the entire 40-ps to 80-ns period does not change (data not shown).

(after ≈30-ps excitation) was the initial evidence suggesting the presence of KL (2). The KL absorption spectrum extracted from these data resembles that of K-590 but has a reduced absorption coefficient and a blue-shifted (10–20-nm) absorption maximum. At 630 nm, the maximum (≈30%) decrease in sample absorbance was reported to occur as KL was formed from K-590 (2). No absorbance change was observed in the 550–580-nm region, suggesting that the absorption spectra of K-590 and KL differ little in this spectral region.

In a subsequent study, a decrease in ΔA was observed in the 600–660-nm region only during the ≈10-ns time resolution (4–7-ns pump pulses and ≈5-ns gated detection) of the measurements (16). No absorbance changes were observed at 625, 590, or 560 nm for time delays between 20 and 100 ns. When these results were viewed within the context of the earlier study (2), it was concluded that KL could appear only within the initial ≈10 ns of the photocycle (16). On the basis of the BR literature, therefore, it was anticipated that the ΔA signal near 630 nm would change by ≈30% within 10 ns, but remain unchanged for a 570-nm probe wavelength.

The PTA data presented here do not agree with the first of these expectations. After the formation of K-590 during the initial 40 ps of the photocycle (initiated by 7-ps excitation), both the 568 and 628 nm PTA signals remain constant from 40 ps to 80 ns (Fig. 2). The same PTA results are obtained for a probe wavelength of 652 nm. Thus, PTA data obtained with 7-ps low energy excitation exhibit no absorbance changes that can be attributed to KL and, therefore, provide no evidence that a K-590 to KL transition occurs during the 40-ps to 80-ns photocycle interval. The constant PTA signals from 40 ps to 80 ns are inconsistent with the earlier literature, which localized the formation of KL (via ≈30% ΔA) in the 500-ps to 10-ns interval (2, 16). Earlier studies did report constant absorbance signals over some time regimes (e.g., from 50 to 500 ps [2] and 10 to 100 ns [16]) but, taken together, these results suggested that KL was present during the 500-ps to 10-ns interval, a conclusion not supported by the PTA data presented here.

The disagreement between the results of the three transient absorption studies are likely attributable to the different excitation conditions used, namely pulsewidths (7 ps [this work] vs. 30 ps [2] vs. 4–7 ns [16]) and pulse energies (10 nJ/pulse [this work], 10 μJ/pulse [2], and 3.0 mJ/pulse [16]). The contrast is especially clear when the resultant photon densities of the pump pulses are considered (0.2 photons/A^2 [this work]; 0.3 photons/A^2 [2]; 4 photons/A^2 [16]). These variations in excitation conditions change the photo-induced mixture of photocycle species (photochemical and photophysical) present at a given time delay and thereby alter the transient absorption signals. For example, 10-ns pulsed excitation produces substantial optical excitation of K-590, which results at least in some reformation of BR-570 (20, 21). The 7-ps pulsed excitation pumps primarily BR-570 since the K-590 population during the pulse is small and the J-625 absorption is shifted far to the red. Analogously, large photon densities increase the probability for multiple excitation of BR-570 during pumping.

Data from a PTR^3 study (23) have been used to suggest that the KL intermediate appears at 10–200 ps. This result, however, disagrees with other PTR^3 studies in which the only intermediate found to be present in the 20-ps to 26-ns interval is K-590 (reference 10 and Brack T., and G. H. Atkinson, unpublished results). These latter PTR^3 studies measured the K-590 RR spectrum as a function of time over the entire 40-ps to 26-ns interval without detecting any significant changes. Differences in subtracting the contribution of ground state BR-570 from the PTR^3 spectra may account for the apparent differences in RR spectra that led to this proposal that KL is formed. It is important to note that there is no evidence from either PTA nor PTRF data to support the appearance of KL within the initial ≈10–200 ps of the photocycle.

PTRF data

The decrease in the PTRF signal over the initial 13 ns (Fig. 3) is not accompanied by any change in the fluorescence spectrum (13, 15 and Brack T., and G. H. Atkinson, unpublished results), indicating that the same K* excited electronic state levels are emitting. The fluores-

cence spectrum remains the same as that reported earlier for K* (13). Since the emitting level(s) are unchanged, the PTRF decrease can be attributed to either differences in the ground state population of K-590 or in the fraction of the K* population created optically that reaches the emitting levels *vide infra.*

Comparison of PTA and PTRF data

The constant PTA signal over the 40-ps to 80-ns interval demonstrates that the ground state K-590 population (as well as that of BR-570) remains unchanged. It is evident from the PTRF data measured over this same time interval, however, that the total fluorescence signal decreases dramatically (Fig. 3). Two explanations should be considered:

First, a new intermediate with substantially smaller fluorescence yield may be formed from K-590. There is no direct evidence to support this conclusion since the fluorescence spectrum measured from the sample remains unchanged except in total intensity (i.e., the same excited electronic state levels are emitting). Alternatively, emission from the proposed new species could appear at a significantly shifted wavelength out of the spectral region observed. This is unlikely given the constant sample absorbance in the visible over the 40-ps to 80-ns interval.

Second, the relaxation properties of K* may be altered during the 40-ps to 80-ns interval resulting in a lower total fluorescence yield. This explanation is consistent with a constant fluorescence spectrum since the K* levels that are emitting remain unchanged and only the amount of fluorescence decreases in response to changes in the competition between radiative and nonradiative decay channels in K*. The fraction of the optically pumped K* population reaching the emitting levels decreases because of the increasing effectiveness of nonradiative decay processes. This explanation also is favored since the comparison of the PTA and PTRF data demonstrates conclusively that the alterations in the excited state properties (fluorescence) are not accompanied by an analogous changes in the ground state (absorption).

The increased effectiveness of nonradiative decay reflected in the decreased K* fluorescence yield can be attributed to time-dependent alterations in retinal–protein interactions. The protein environment near the retinal chromophore when K-590 is initially formed during the first 40 ps of the photocycle does not remain fixed, but rather changes over the next 13 ns with a time constant of $\approx$5.5 ns. Such changes could involve alterations in the relative distances between specific parts of the protein and retinal and/or in their respective charged properties. Both types of changes could influence the decay properties of K* and thereby alter the amount of K* fluorescence. The K* fluorescence spectrum would remain unchanged.

This interpretation can be readily tested with PTA and PTRF studies analogous to those described here in which the protein and retinal structures are systematically controlled. BR mutants (e.g., where ASP 85 is exchanged) in which the amino acids comprising the protein environment adjacent to the retinal chromophore are systematically replaced can be used to probe the chromophore–protein interactions. Analogously, PTA and PTRF measurements of artificial BR pigments containing different structurally modified retinal chromophores (e.g., 13-demethylretinal [27–29]) can be used to examine the influence of retinal properties. Taken together, these studies should identify the specific retinal–protein interactions that control the K* fluorescence and thereby characterize the physical interactions involved. Given the recognized importance of both the retinal and protein to the BR photocycle, it is evident that such interactions may fulfill critical roles in the overall biochemical functionality of BR.

We acknowledge Daniel Hughes and Peter Schmidt for technical assistance.

This research was supported by a grant from the National Science Foundation.

Received for publication 12 August 1992 and in final form 26 January 1993.

REFERENCES

1. Lozier, R. H., R. Boglomoni, and W. Stoeckenius. 1975. Bacteriorhodopsin: a light-driven proton pump in *Halobacterium halobium. Biophys. J.* 15:955–962.
2. Shichida, Y., S. Matuoka, Y. Hidaka, and T. Yoshizawa. 1983. Absorption spectra of intermediates of Bacteriorhodopsin measured by laser photolysis at room temperatures. *Biochim. Biophys. Acta.* 723:240–246.
3. Polland, H.-J., M. A. Franz, W. Zinth, W. Kasier, E. Kolling, and D. Oesterhelt. 1986. Early events in the photocycle of bacteriorhodopsin. *Biophys. J.* 49:651–662.
4. Blanchard, D., D. A. Gilmore, T. L. Brack, H. Lemaire, and G. H. Atkinson. 1991. Picosecond time-resolved absorption and fluorescence spectroscopy in the bacteriorhodopsin photocycle. *Chem. Phys.* 154:155–170.
5. Atkinson, G. H. 1982. Time resolved Raman spectroscopy. *In* Advances in Infrared and Raman spectroscopy. Vol. 9. R. J. H. Clark and R. E. Hester, editors. North-Holland Publishers, London. 1–62.
6. Hsieh, C. L., M. A. El-Sayed, M. Nicol, M. Nagumo, and J.-H. Lee. 1983. Time resolved resonance Raman spectroscopy of the bacteriorhodopsin photocycle on the picosecond and nanosecond time scales. *Photochem. Photobiol.* 38:83–94.
7. Smith, S. O., M. Braiman, and R. Mathies. 1983. Time-dependent resonance Raman spectroscopy of the K_{610} and O_{640} photointermediate of bacteriorhodopsin. *In* Time-resolved Vibrational Spectroscopy. G. H. Atkinson, editor. Academic Press, New York. 219–230.
8. Stern, D., and R. Mathies. 1985. Picosecond and nanosecond resonance Raman evidence for structural relaxation in bacterio-rhodopsin's primary photoproduct. *In* Time-resolved Vibrational Spectroscopy. Vol. 4. A. Laubereau and M. Stockburger, editors. Springer-Verlag, New York. 250–254.
9. Stockburger, M., T. Alshuth, D. Oesterhelt, and W. Gartner. 1986.

Resonance Raman spectroscopy of bacteriorhodopsin: structure and function. *In* Advances in Infrared and Raman Spectroscopy. Vol. 13. R. J. H. Clark and R. E. Hester, editors. John Wiley & Sons, Inc., New York. 483–535.

10. Brack, T., and G. H. Atkinson. 1989. Picosecond time-resolved resonance Raman spectrum of the K-590 intermediate in the room temperature bacteriorhodopsin photocycle. *J. Mol. Struct.* 214:289–303.
11. Braiman, M. S., T. Mogi, T. Marti, L. Stern, H. G. Khorana, and K. J. Rothschild. 1988. Vibrational spectroscopy of bacteriorhodopsin mutants: light-driven proton transport involves protonation changes of aspartic acid residues 85, 96 and 212. *Biochemistry.* 27:8516–8521.
12. Fahmy, K., F. Siebert, M. F. Grobjean, and P. Taven. 1989. Photoisomerization in BR studied by FTIR, linear dichroism and photoselection experiments combined with quantum chemical theoretical analysis. *J. Mol. Struct.* 214:257–288.
13. Atkinson G. H., T. L. Brack, D. Blanchard, and G. Rumbles. 1989. Picosecond time-resolved fluorescence spectroscopy of K-590 in the bacteriorhodopsin photocycle. *Biophys. J.* 55:263–274.
14. Blanchard, D., D. A. Gilmore, T. L. Brack, H. Lemaire, and G. H. Atkinson. 1991. Picosecond time-resolved absorption and fluorescence spectroscopy in the bacteriorhodopsin photocycle. *Chem. Phys.* 154:155–170.
15. Atkinson, G. H., D. Blanchard, and T. L. Brack. 1991. Fluorescence from the primary products of the bacteriorhodopsin photocycle. *J. Lumin.* 48 & 49:410–414.
16. Milder, S. J., and D. S. Kliger. 1988. A time resolved spectral study of the K and KL intermediates of bacteriorhodopsin. *Biophys. J.* 53:465–468.
17. Diller, R., and M. Stockburger. 1988. Kinetic resonance Raman studies reveal different conformational states of bacteriorhodopsin. *Biochemistry.* 27:7641–7651.
18. Varo, G., and J. K. Lanyi. 1990. Pathways of the rise and decay of the M photointermediate(s) of bacteriorhodopsin. *Biochemistry.* 29:2241–2250.
19. Goldsmidt, C. R., M. Ottolenghi, and R. Korenstein. 1976. On the primary quantum yields in the bacteriorhodopsin photocycle. *Biophys. J.* 16:839–843.
20. Govindjee, R., S. P. Balashov, and T. G. Ebery. 1990. Quantum efficiency of the photochemical cycle of bacteriorhodopsin. *Biophys. J.* 58:597–607.
21. Bazhenov, V., P. Schmidt, and G. H. Atkinson. 1992. Nanosecond photolytic interruption of bacteriorhodopsin photocycle. K-590 → BR-570 reaction. *Biophys. J.* 61:1630–1637.
22. Ebrey, T. G. 1992. Light energy transduction in bacteriorhodopsin. *In* Thermodynamics of Cell Surface Receptors. M. Jackson, editor. CRC Press, Boca Raton, Florida.
23. Doig, S. J., Reid, P. J., and R. A. Mathies. 1991. Picosecond time-resolved resonance Raman spectroscopy of bacteriorhodopsin's J, K, and KL intermediates. *J. Phys. Chem.* 95:6372–6379.
24. Lewis, A., J. P. Spoonhower, and G. J. Perreault. 1976. Observation of light emission from a rhodopsin. *Nature (Lond.).* 260:675–678.
25. Oesterhelt, D., and W. Stoeckenius. 1974. Isolation of the cell membrane of *Halobacterium halobium. Methods Enzymol.* 31:667–671.
26. Shinar, R., S. Druckmann, M. Ottolenghi, and R. Horenstein. 1977. Electric field effects in bacteriorhodopsin. *Biophys. J.* 19:1–5.
27. Trissl, H.-W., and W. Gartner. 1987. Rapid charge separation and bathochromic absorption shift of flash excited bacteriorhodopsins containing 13-cis of all trans forms of substituted retinals. *Biochemistry.* 26:751–758.
28. Zinth, W., J. Dobler, M. A. Franz, and W. Kaiser. 1988. The primary steps of photosynthesis in bacteriorhodopsin. *In* Spectroscopy of Biological Molecules—New Advances. E. Schmid, F. W. Schneider, and F. Siebert, editors. John Wiley & Sons, Inc., New York. 269–274.
29. Brack, T. L., W. Gartner, and G. H. Atkinson. 1992. Picosecond time-resolved fluorescence spectroscopy of 13-demthylretinal bacteriorhodopsin. *Chem. Phys. Lett.* 190:298–304.